Numerical Simulation of Wear Process on Inductively Hardened Sample Exposed to Rolling Contact

ŠOFER Michal[1,a], HALAMA Radim[1,b] and FAJKOŠ Rostislav[1,c]

[1]VŠB-TU Ostrava, 17. listopadu 15/2127, 708 33 Ostrava-Poruba, Czech Republic

[a]michal.sofer@vsb.cz, [b]radim.halama@vsb.cz, [c]rostislav.fajkos@vsb.cz

Keywords: Rolling contact fatigue, wear, ratcheting.

Abstract. Presented paper deals with ratcheting prediction in the field of line rolling contact. The main aim is to simulate the wear process due to the contact fatigue on inductively hardened sample of R7T material. For the stated purposes, the authors have used the wear model based on shear band cracking mechanism and non-linear kinematic and isotropic hardening rule of Chaboche and Lemaitre. Obtained results are subsequently compared with experimental data as well as with metallographic analysis.

Introduction

Description of the interaction between rail and wheel is even today still very complex set of problems to be described. We have to take into account phenomena such as hardening of the material in the surface and subsurface layers and also the crack propagation mechanism 0.

The prevailing wear mechanism in case of dry rolling/sliding contact is undoubtedly ratcheting, which is, among other, responsible for plastic deformation accumulation below contact surface. Fletcher and Beynon observed equilibrium between wear and crack growth 0. The crack growth, in itself, can be described by two phases: initiation of crack as the result of ratcheting and its propagation by the effect of shear stress. Tyfour et al. observed, that reaching the accumulated critical plastic deformation in particular depth is a starting point of a crack initiation phase 0.

In most cases, nucleated cracks grow parallel to the contact surface and cause material delamination (flanking phenomena, see Fig. 1) 0. According to Merwin and Johnson 0 the orthogonal shear strain γ_{xz} is the only component responsible for accumulation of plastic shear strain below contact surface.

Fig. 1. Flanking phenomena.

Nowadays, despite the possibility of using relatively powerful computers, are the semi-analytical approaches still powerful tools for wear and ratcheting prediction.

One of them is the approach of A. Mazzu 0, who has in his wear model utilized a simplified non-linear kinematic hardening model, based on the Chaboche-Lemaitre plasticity model. According to Mazzu, the only stress component, responsible for plastic flow is τ_{xz}. Proposed hypothesis is, however, not valid at shallow depths below the contact surface, where σ_x stress component plays a major role on plastic shear accumulation (Fig. 5). One year later, Mazzu therefore published a correction of his algorithm 0, which takes into account the influence of σ_x stress component at shallow depths below the contact surface.

Proposed paper presents a new way of ratcheting and wear prediction based on the results from experiment on inductively hardened R7T material. The elastic stress field, which is needed for following numerical computations with the semi-analytical approach 0, is originally obtained with use of Boussinesq approximation. Realized numerical computations also take into account the variation of traction coefficient, obtained from realized experimental test. The authors have also, in contrast to 0, applied a new procedure for identifying the Chaboche plasticity model material parameters. The procedure is based on an algorithm with a random number generator. All procedures have been written in C# programming language.

Rolling Contact Fatigue Test

The rolling contact wear test has been performed in the Rolling Contact Fatigue Laboratory at the Department of Mechanics of Materials of VŠB - Technical University of Ostrava, using the TUORS testing machine 0, see Fig. 2. The diameter of the wheel disc was 82,45 mm, whereas the diameter of the rail disc was 215,55mm. The wheel specimen was made of R7T steel and was subsequently heat treated by induction hardening. The rail specimen was made of class C steel.

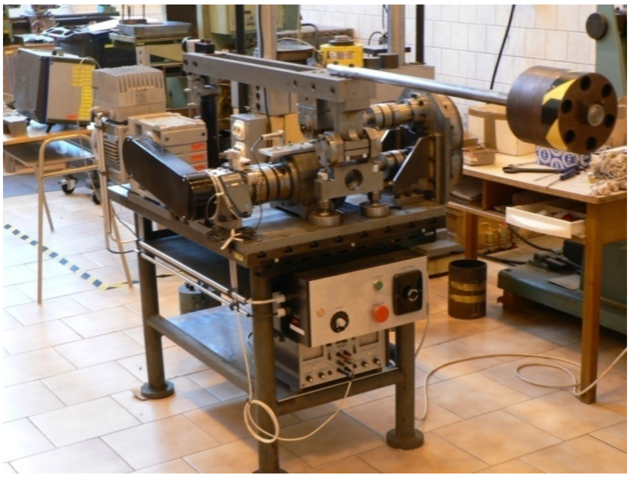

Fig. 2. TUORS testing machine.

The difference between the diameters of the specimen and the diameters of the gears in the gearbox led to creepage of 0,75 %. The Hertzian contact pressure was 1200 MPa and the wheel specimen realized 10^5 cycles in total. The torque has been recorded during the entire test on the shaft, which has been carrying the wheel specimen. For selected number of cycles (10000, 20000, 60000 and 100000) has the test procedure been stopped and we have measured the weight and diameter loss as well as the roughness of the contact surface of the wheel specimen. Furthermore, a photographic documentation of the contact surface has been made. Table 1 summarizes the values of computed loss of radius, which has been stated according to the measured weight loss. Fig. 3 displays the torque record on the shaft, which has been carrying the wheel specimen, for the first 5000 cycles. The value of the torque become stabilized on the mean value of 153 N·m after 4800 cycles and remained stable until the end of the test (10^5 cycles).

Table 1. Computed loss of radius.

Number of cycles [-]	Loss of radius [mm]
10000	0,0006
20000	0,011
60000	0,049
100000	0,148

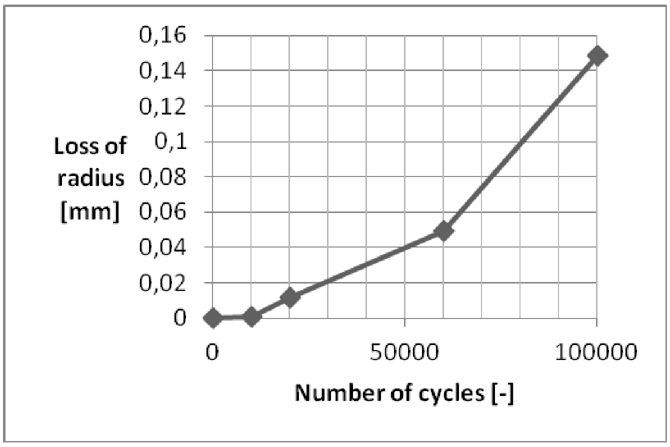

Fig. 3. Worn depth as the function of number of cycles.

Metallographic Analysis

After 10^5 cycles, the wheel specimen has been subjected to metallographic analysis, focused on evaluation of critical value of plastic shear strain (γ_{crit}) and shape of the deformation profile below contact surface. Following picture shows us the methodology of determining the critical plastic shear strain, which is proportional to the slope of the tangent corresponding to the plastic flow orientation at the crack tip 0, see Fig. 5.

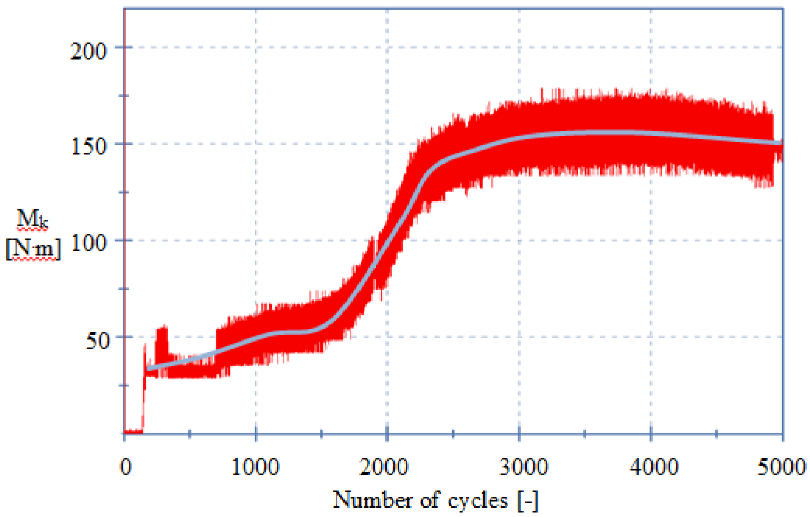

Fig. 4. Torque record for the first 5000 cycles.

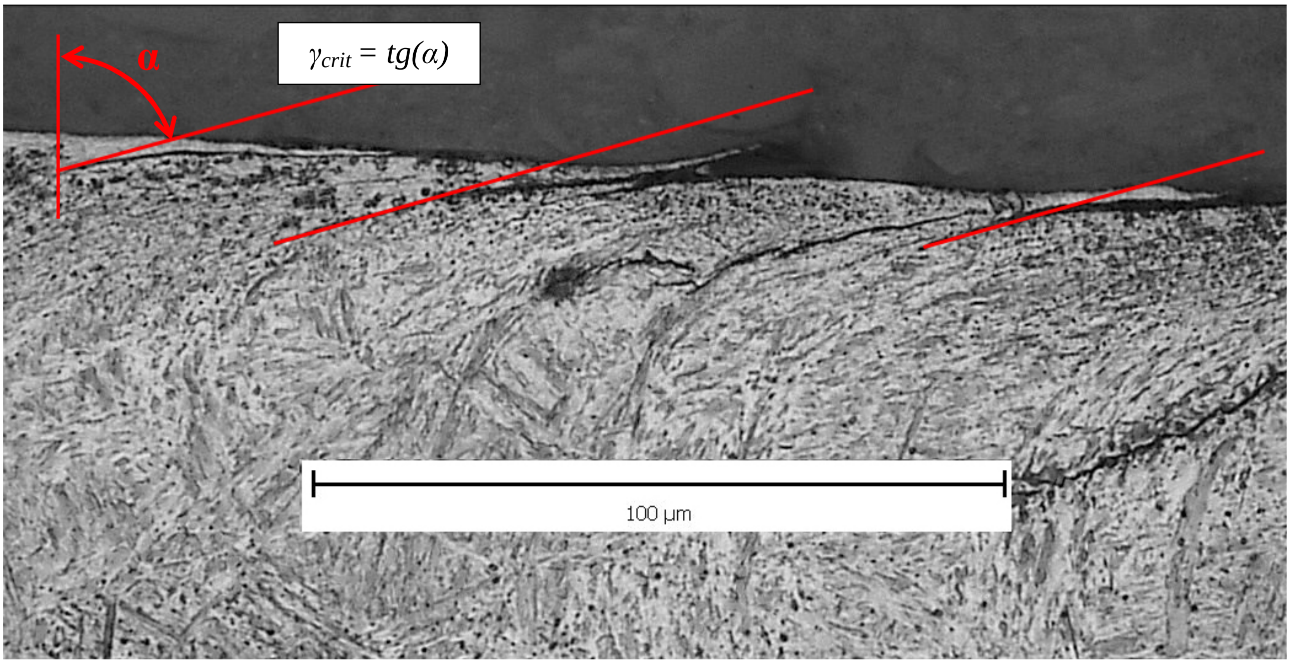

Fig. 5. Evaluation of critical plastic shear deformation.

The mean value of angle, representing the plastic flow orientation at the crack tip, was equal to 73,6 degrees, which corresponds to γ_{crit} = 3,41 [-].

Wear Model

Applied wear model is based on, so called, shear band cracking mechanism. The mechanism describes the wear process as independent simultaneous phenomenon, responsible for removing the layers of the material from the surface as a result of plastic shear strain accumulation below the contact surface. Surface initiated cracks follow the plastic lines according to the presence of ductility exhaustion 0.

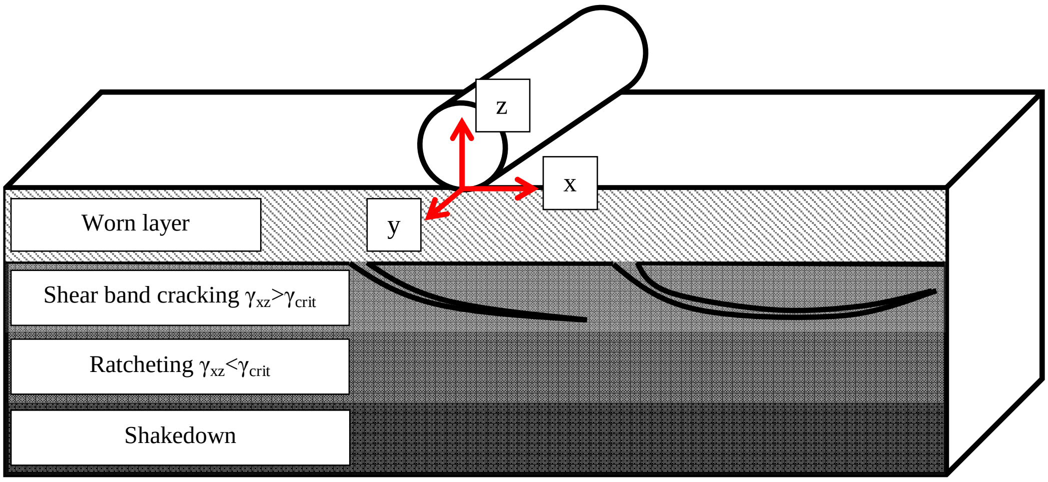

Fig. 6. Shear band cracking mechanism.

For ratcheting prediction in particular depths below contact surface in case of rolling/sliding two-dimensional contact, the authors have used a non-linear kinematic hardening rule, introduced by Lemaitre and Chaboche 0 (see Table 1), which is described in detail in 0. Unlike Mazzu 0, we have used two Voce rules, which allow us to control the entire hardening process more flexibly. The numerical simulations also took into account the variability of coefficient of friction, which played an important role in the evolution of ratcheting in the first 5000 cycles (see Fig. 4). Every ten cycles, there has been realized an update of elastic stress field according to the value of friction coefficient, which has been derived from the torque record. Beyond 5000 cycles, the value of friction coefficient become a constant (f = 0,39 [-]).

Table 1. Chaboche-Lemaitre plasticity model.

Elastic domain definition	$F=\left\lvert\sqrt{3}\cdot\tau_{xz}-X_{xz}\right\rvert-(R+\sigma_L)\le 0$
Back-stress variation law	$dX_{xz}=C\cdot\frac{d\gamma_{xz}}{\sqrt{3}}-\gamma\cdot X_{xz}\cdot\left\lvert\frac{d\gamma_{xz}}{\sqrt{3}}\right\rvert$
Isotropic term variation law	$R=R_{\infty 1}\cdot\left[1-\exp\left(-b_1\cdot\frac{\gamma_{xz}}{\sqrt{3}}\right)\right]+R_{\infty 2}\cdot\left[1-\exp\left(-b_2\cdot\frac{\gamma_{xz}}{\sqrt{3}}\right)\right]$
Evaluation of back-stress variable between two steps	$X_{xz}=\nu\cdot\frac{C}{\gamma}+\left(X_{xz}^0-\nu\cdot\frac{C}{\gamma}\right)\exp\left[-\frac{\nu\cdot\gamma}{\sqrt{3}}\cdot\left(\gamma_{xz}-\gamma_{xz}^0\right)\right]$
Plastic shear strain increment	$\Delta\gamma_{xz}=-\frac{\sqrt{3}}{\nu\cdot\gamma}\cdot\ln\left[\frac{X_{xz}-\nu\cdot(C/\gamma)}{X_{xz}^0-\nu\cdot(C/\gamma)}\right]$

Calibration of Chaboche Plasticity Model

The material parameters for further calculations of the deformation profiles were obtained with aim of numerical approach, which has been developed by authors themselves. Due to the nature of the task, we were not able to use an optimization algorithm, which would incorporate a particular gradient method. The reason was, that the parameters are extremely varying on each other, so that we would not be able to find the minimum of the complex function with optional mathematical and physical interpretation. Therefore, we have incorporated a random number generator, which generates in each step a unique set of parameters.

The optimization procedure starts by defining the intervals for each parameter from which the random numbers have to be generated. The random number generator works on the basis of generating numbers with uniform distribution pattern. One cycle contains four computations of wear layer under prescribed reference number of cycles, afterwards an error value is evaluated in following way

$$error^{i} = \sum_{k=1}^{4}\left(\frac{\left|h_{Wref\ k} - h_{W}{}^{k}\right|}{h_{Wref\ k}}\right), \tag{1}$$

where $h_{Wref\ k}$ is the reference value of the worn layer and $h_W{}^k$ is the value of worn layer reached after specified number of cycles. Reference values of the worn layer with corresponding value of cycles were obtained from realized experiment. Following table summarizes obtained material parameters for Chaboche plasticity model as well as supportive data, needed for numerical simulation.

Table 2. Parameters for semianalytical simulation.

<table>
<tr><td colspan="2" rowspan="2">Reference values of worn layer with corresponding value of number of cycles obtained from experiment</td><td rowspan="7">Material parameters</td><td>C [MPa]</td><td>230 000</td></tr>
<tr><td>γ [-]</td><td>0,6</td></tr>
<tr><td>Worn layer [mm]</td><td>Number of cycles [-]</td><td>σ_L [MPa]</td><td>560</td></tr>
<tr><td>0,0006</td><td>10 000</td><td>$R_{\infty 1}$ [MPa]</td><td>30</td></tr>
<tr><td>0,011</td><td>20 000</td><td>b_1 [-]</td><td>0.1</td></tr>
<tr><td>0,049</td><td>60 000</td><td>$R_{\infty 2}$ [MPa]</td><td>10</td></tr>
<tr><td>0,148</td><td>100 000</td><td>b_2 [-]</td><td>0,0001</td></tr>
<tr><td colspan="2" rowspan="2">Line contact parameters</td><td colspan="2">Maximal Hertz contact pressure p_0 [MPa]</td><td>1 200</td></tr>
<tr><td colspan="2">Hertz contact half width a [mm]</td><td>0,71</td></tr>
<tr><td colspan="2" rowspan="3">Other parameters</td><td colspan="2">Range of inspected depths z_{min} - z_{max} [mm]</td><td>0,0006- 0,15</td></tr>
<tr><td colspan="2">Number of layers in the range of inspected depths</td><td>250</td></tr>
<tr><td colspan="2">Critical plastic shear deformation γ_{crit} [-]</td><td>3,41</td></tr>
</table>

Results

A total of four computations were made with aim to obtain the plastic shear deformation profile below worn layer as well as to assess the loss of radius after $1 \cdot 10^4$, $2 \cdot 10^4$, $6 \cdot 10^4$ and $1 \cdot 10^5$ numbers of cycles. As mentioned earlier, the experiment has been for specified numbers of cycles interrupted in order to obtain the weight loss and other needful data. According to the Fig. 7, where are displayed computed plastic shear deformation profiles, we can say, that the stabilization process of the profile was held earlier than in 10000 cycles. This phenomenon is directly bounded to the presence of material layer which underwent some type of heat treatment. The harder the surface and subsurface material layers are, the less number of cycles is needed for stabilization of deformation profile. From Fig. 7 we can also notice the bound of the active layer in which occurs in dominant way the accumulation process of plastic shear deformation.

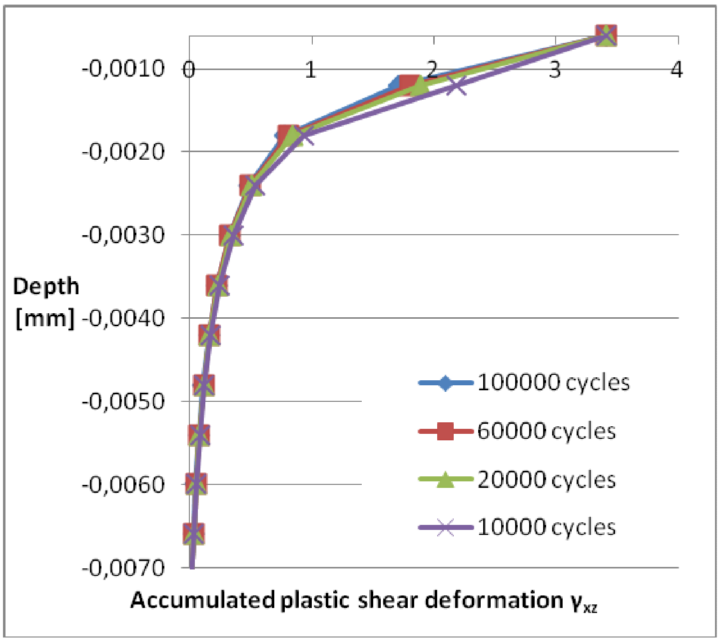

Fig. 7. Accumulated plastic shear strain profiles.

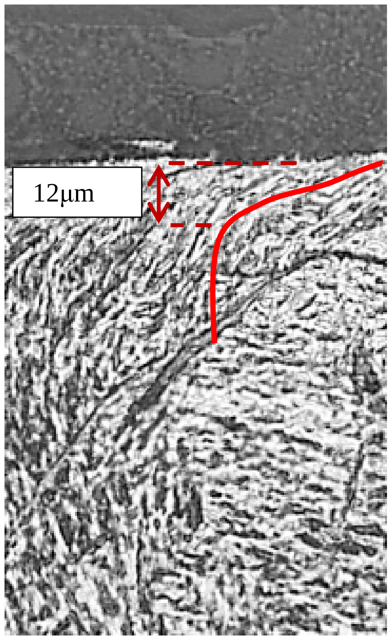

Fig. 8. Metallographic analysis of deformation profile.

The thickness of active layer was in case of numerical simulation equal to 7 micrometers, while the metallographic analysis showed the mean value of 12 micrometers. Fig. 9 displays dependence of loss of radius on the number of cycles. It can be clearly seen, that the presented wear model tends to predict the loss of diameter linearly compared to experimental data. The conformity between the experiment and the numerical simulation was acceptable taking into account that we are operating in a very shallow depths below contact surface. Thanks to relatively low critical plastic shear deformation and as mentioned before, shallow depths below contact surface, is the entire process of finding and optimizing the material parameters very sensitive and challenging as well.

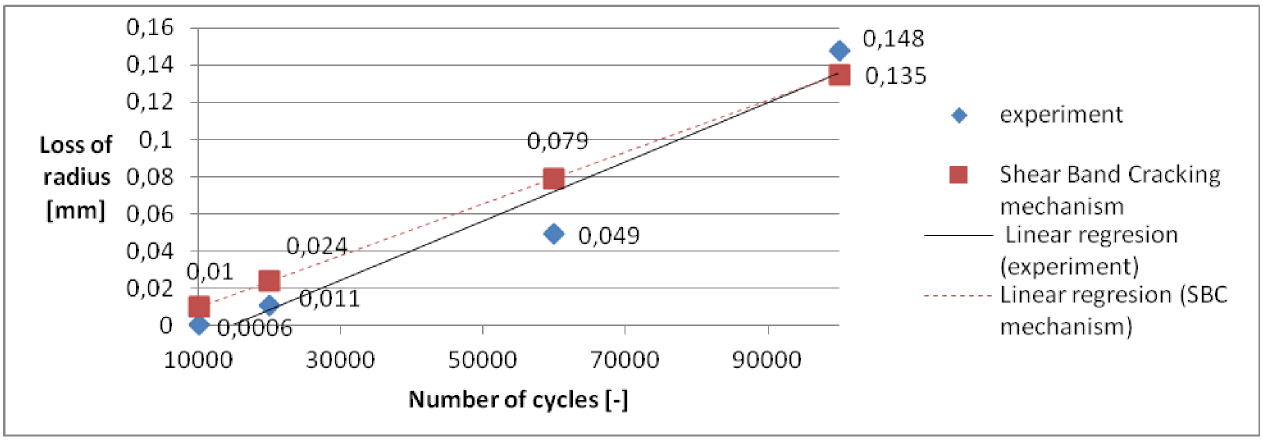

Fig. 9. Loss of radius as the function of number of cycles.

Conclusion

A wear model, based on shear band cracking mechanism and ratcheting prediction by use of a non-linear kinematic hardening rule, introduced by Lemaitre and Chaboche 0, enables not only to determine the wear rate for particular loading conditions, but also, and especially, to analyze and assess the evolution of the accumulation of plastic shear strain beneath the contact surface. Overall, four numerical simulations have been realized in order to determine the loss of radius as well as the deformation profile below contact surface. Numerically obtained values of loss of radius were afterwards compared with their counterparts, calculated from weight loss (Fig. 9). The comparison between the numerical solution and experimental data in case of loss of radius and the thickness of active layer showed relatively good agreement between these two approaches taking into account that we are operating in a very shallow depths below contact surface. From engineering point of view, the wear model can be used for evaluation of wear resistance in different kinds of practical applications.

Acknowledgment

This work has been elaborated in the framework of the project Opportunity for young researchers, reg. no. CZ.1.07/2.3.00/30.0016, supported by Operational Programme Education for Competitiveness and co-financed by the European Social Fund and the state budget of the Czech Republic and in the framework of the IT4Innovations Centre of Excellence project, reg. no. CZ.1.05/1.1.00/02.0070, supported by Operational Programme Research and Development for Innovations and funded from the Structural Funds of the European Union.

References

[1] G. Donzella, M. Faccoli, A. Mazzu, C. Petrogalli, R. Roberti, Progressive damage assessment in the near-surface layer of railway wheel-rail couple under cyclic contact, Wear 271 (2011) 408-416.

[2] D.I. Fletcher, J.H. Beynon, Equilibrium of crack growth and wear rates during unlubricated rolling-sliding contact of pearlitic rail steel, Proceedings of the Institution of Mechanical Engineers Part F 214 (2000) 93-105.

[3] W.R. Tyfour, J.H. Beynon, A. Kapoor, Deterioration of rolling contact fatigue life of pearlitic rail due to dry-wet rolling–sliding line contact, Wear 197 (1996) 255-265.

[4] A. Kapoor, F.J. Franklin, Tribological layers and the wear of ductile materials, Wear 245 (2000) 204–215.

[5] O. Umezawa, S. Morooka, J. Brumek, Subsurface crack generation and flaking under rolling contact fatigue, in: Proceedings of Workshop New Methods and Failure Analysis of Structural Parts, Ostrava, 2012, pp. 421-427.

[6] J.E. Merwin, K.L. Johnson, An analysis of plastic deformation in rolling contact, Proceedings of the Institution of Mechanical Engineers 177 (1963) 676-685.

[7] A. Mazzu, A simplified non-linear kinematic hardening model for ratcheting and wear assessment in rolling contact, Journal of Strain Analysis 43 (2008) 349-360.

[8] A. Mazzu, Surface plastic strain in contact problems: prediction by a simplified non-linear kinematic hardening model, Journal of Strain Analysis 44 (2009) 187-199.

[9] R. Halama, R. Fajkoš, P. Matušek, P. Bábková, F. Fojtík, L. Václavek, Contact defects initiation in railroad wheels – Experience, experiments and modeling, Wear 271 (2011) 174-185.

[10] X. Su, P. Clayton, Surface initiated rolling contact fatigue of pearlitic and low carbon bainitic steels, Wear 197 (1996) 137-144.

[11] J. Lemaitre, J.L. Chaboche, Mechanics of solid materials, Cambridge University Press, Cambridge, 1994.